Investigation of the ^{241}Am$(n,2n)^{240}$Am cross section

A. Kalamara,[1,*] R. Vlastou,[1] M. Kokkoris,[1] M. Diakaki,[1,†] A. Tsinganis,[1,‡] N. Patronis,[2] M. Axiotis,[3] and A. Lagoyannis[3]

[1]*Department of Physics, National Technical University of Athens, 15780 Athens, Greece*

[2]*Department of Physics, University of Ioannina, 45110 Ioannina, Greece*

[3]*Institute of Nuclear and Particle Physics, NCSR "Demokritos", 15310 Aghia Paraskevi, Greece*

(Received 13 November 2015; published 14 January 2016)

The ^{241}Am$(n,2n)^{240}$Am reaction cross section has been measured at four energies, 10.0, 10.4, 10.8, and 17.1 MeV, by means of the activation technique, relative to the ^{27}Al$(n,\alpha)^{24}$Na reaction reference cross section. Quasi-monoenergetic neutron beams were produced via the ^{2}H$(d,n)^{3}$He and the ^{3}H$(d,n)^{4}$He reactions at the 5.5 MV Tandem T11/25 accelerator laboratory of NCSR "Demokritos". The high purity ^{241}Am targets were provided by JRC-IRMM, Geel, Belgium. The induced γ-ray activity of ^{240}Am was measured with high-resolution high-purity germanium (HPGe) detectors. Auxiliary Monte Carlo simulations were performed with the MCNP code. The present results are in agreement with data obtained earlier and predictions obtained with the EMPIRE code.

DOI: 10.1103/PhysRevC.93.014610

I. INTRODUCTION

The determination of (n,xn) reaction cross sections is important for the development of fast reactors, since the neutron balance in the core of the reactor is affected by the neutron multiplication caused by such reactions. However, the existing experimental data concerning the actinides present many experimental difficulties, with the considerable natural activity of the samples and the limited availability of high-purity materials being the most significant ones. More specifically, the study of the ^{241}Am$(n,2n)$ reaction is important, as Am is one of the most radiotoxic isotopes among the actinides and one of the most abundant components of spent nuclear fuel. Therefore, accurate cross section data are needed for many practical applications, especially in the field of nuclear energy and transmutation of radioactive waste.

Several recent works provide data for the ^{241}Am$(n,2n)$ reaction, from threshold to 20 MeV [1–5]. The data of Lougheed *et al.* [2] and Tonchev *et al.* [4] around 14 MeV, are in good agreement, while the data by Filatenkov *et al.* [1] are systematically lower by approximately two standard deviations. The data by Perdikakis *et al.* [3], which have been measured at NCSR "Demokritos", agree well with the data of both Tonchev *et al.* [4] and Sage *et al.* [5] below 10 MeV. There are, however, severe discrepancies between the measurements of Refs. [3] and [4] in the energy region between 10 to 12 MeV.

In this work, in order to resolve these discrepancies between the existing data, the cross section of the ^{241}Am$(n,2n)^{240}$Am reaction has been measured in the incident neutron energy range between 10.0 and 17.1 MeV, with a high-purity Am target provided by IRMM, implementing the activation technique. Additionally, theoretical statistical model calculations were performed and compared to all available experimental data.

II. EXPERIMENTAL PROCEDURE

A. Irradiation setup

The ^{241}Am$(n,2n)^{240}$Am reaction cross section has been measured at four energies in the range between 10.0 and 17.1 MeV, by means of the activation technique, relative to the ^{27}Al$(n,\alpha)^{24}$Na reaction reference cross section, while results were cross-checked using the ^{197}Au$(n,2n)^{196}$Au and ^{93}Nb$(n,2n)^{92m}$Nb reference reactions. The irradiations were carried out at the 5.5 MV Van de Graaff Tandem T11/25 accelerator laboratory of NCSR "Demokritos".

First, quasi-monoenergetic neutrons with energies of 10.0, 10.4, and 10.8 MeV were produced via the ^{2}H$(d,n)^{3}$He reaction ($Q = 3.269$ MeV) at $E_d = 7.2$, 7.6, and 8.0 MeV, respectively, using a deuterium gas target. The gas target consisted of a stainless steel gas cell, 3.7 cm in length and 1 cm in diameter, with a 5 μm molybdenum foil serving as the entrance window and a 2 mm platinum foil serving as the beam stop. During the irradiations, the gas cell was air cooled at the position of the Mo window and the Pt beam stop. Thus, the heat transferred on the gas target by the deuteron beam, was dissipated effectively, in order to reduce the effect of heating on the deuterium gas pressure. The pressure in the cell was kept under 130 kPa. The samples were placed ∼7 cm from the gas target, thus limiting the angular acceptance of the target and reference foils to ±5° with respect to the deuteron beam axis, where the produced neutrons are expected to be practically monoenergetic according to the reaction kinematics.

Second, quasi-monoenergetic neutrons with an energy of 17.1 MeV were produced via the ^{3}H$(d,n)^{4}$He reaction ($Q =$ 17.59 MeV). The deuterons were accelerated to an energy of 2.5 MeV in order to have sufficient intensity (∼1 μA). Then they passed through two molybdenum foils of 5 μm thickness each, in order to lose a part of their energy, and

*akalamara@central.ntua.gr

†Also at CEA/Sarlay-DSM, Gif-Sur-Yvette, France.

‡Also at CERN, Geneva, Switzerland.

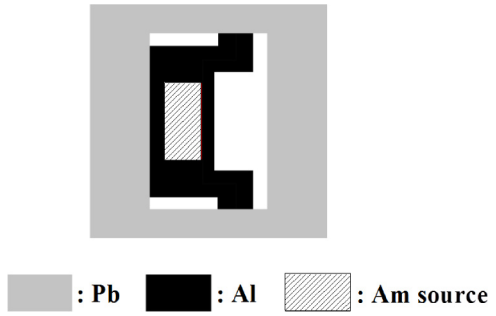

FIG. 1. Schematic diagram of the Am target assembly.

finally impinged on a solid Ti-tritiated target, consisting of a 2.1 mg/cm^2 Ti-tritiated layer on a 1 mm thick Cu backing for good heat conduction. In addition, the flange with the tritium target assembly was air cooled during the deuteron irradiation. The sample was placed at a distance of ∼2 cm from the tritium target, thus limiting the angular acceptance of the target and reference foils to ±15°, where the produced neutrons are expected to be practically monoenergetic according to the reaction kinematics.

The typical beam current on the target was 1–3 μA with a typical neutron flux of 5×10^5–10^6 n/cm^2 s. During the irradiations, each of which lasted 3 days on average, the neutron beam was monitored by a BF_3 detector placed 3 m from the neutron source. The output of the BF_3 detector was stored at regular time intervals by means of a multichannel scaler and was used to correct for the decay of product nuclei during irradiation and to account for fluctuations in the beam flux in the subsequent offline analysis.

Two Am targets (IRMM2 and IRMM3) in the form of AmO_2 pressed into pellets with Al_2O_3 and encapsulated into Al containers, have been provided by JRC-IRMM, Belgium, coming from the same batch of targets used by Sage *et al.* [5]. The IRMM2 target consisted of 42 mg Am and was irradiated with 10.8 MeV neutrons and the IRMM3 target consisted of 40 mg Am and was irradiated with the remaining neutron beam energies 10.0, 10.4, and 17.1 MeV. Due to their high radioactivity, the Am samples (∼5 GBq), were placed inside a 3 mm lead cylindrical shielding (Fig. 1). Moreover, high-purity aluminum foils were placed at the front and back of the Am target, along with Au and Nb foils at the back, to monitor the neutron flux and to account for its variation with distance.

B. Neutron energy and flux determination

The study of the neutron energy spectra generated by deuterons on the gas cell and the Ti-tritium target was carried out using the NEUSDESC code, developed at IRMM [6]. The program takes into consideration the energy loss, energy spread, and angular straggling of the deuterons in the target assembly through the Monte Carlo simulation program SRIM-2008 and calculates average neutron energies, fluences, and resolutions [7]. In the case of the gas cell, the simulations take into account only the entrance Mo foil and the length and pressure of the gas while, for the tritium case only Ti and T are considered. The deuteron breakup reaction ^{2}H(d,np)^{2}H appears as a competing reaction to the ^{2}H(d,n)^{3}He reaction

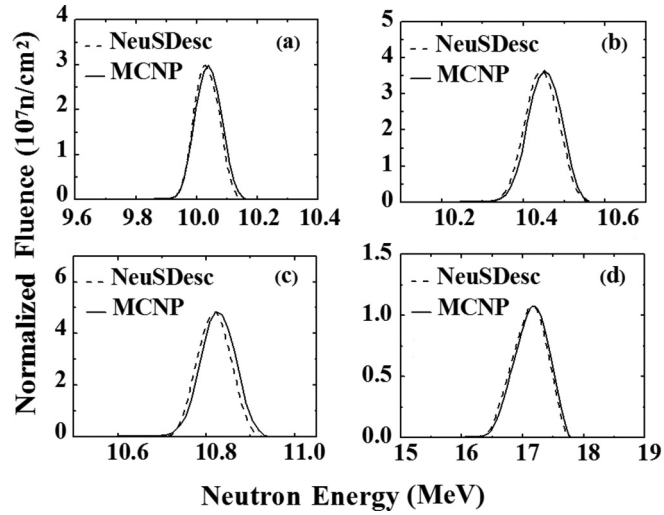

FIG. 2. Neutron energy spectra calculated with NEUSDESC and MCNP5 at the distance of interest either from the gas or from the tritium target for each irradiation: (a) 10.0 ± 0.1 MeV, (b) 10.4 ± 0.1 MeV, (c) 10.8 ± 0.1 MeV, (d) 17.1 ± 0.3 MeV.

and the double differential cross section and kinematics of the ^{3}H(d,n)^{4}He reaction are also used. The results for the average neutron energies, fluences, and energy spreads at the distance of the first Al reference foil used in this work are shown as dashed lines in Fig. 2.

The NEUSDESC program includes the option of creating an MCNP [8] input file containing the description of the neutron field at an arbitrary surface in space. This input file has been used for MCNP5 [9] simulations to investigate the influence on the average neutron energy and resolution due to the Pt foil for the gas cell, and due to the Cu backing and Al flange for the Ti-tritiated target. The results of the MCNP5 simulations are shown as solid lines in Fig. 2 and are seen to be in good agreement with the results from the NEUSDESC code.

MCNP5 simulations were also carried out in order to investigate the neutron fluence by taking into account the detailed geometry of the Am target and its lead shielding, as well as the Al holder and reference foils. The simulated fluences reproduce fairly well the experimentally deduced neutron fluences at the back foils. Therefore, the simulated fluence in the Am pellet was used to determine the cross section. The results of the experimental and simulated fluence values for the 10.4 MeV irradiation are shown in Table I.

C. Induced activity measurements

Following the irradiations both the target and the reference foils were placed at 10 cm from the window of four high-purity germanium (HPGe) detectors, with 100%, 80%, 56%, and 16% relative efficiency, properly shielded with lead blocks in order to reduce the contribution of the natural radioactivity. With this counting setup, any corrections for pile-up or coincidence summing effects were negligible. For the Am targets, γ-ray spectra were also taken before irradiations, to ensure that there was no contamination in the 987.8 keV photopeak from the decay of the ^{240}Am residual nucleus. Two spectra taken before

TABLE I. Experimental and simulated integrated neutron flux at 10.4 MeV.

Target	Experimental neutron fluence Φ ($\times 10^{11}$ n/cm^2)	Neutron fluence from MCNP simulations Φ ($\times 10^{11}$ n/cm^2)
Al front	2.19 ± 0.10	2.19
Am		1.89
Al back	1.50 ± 0.07	1.49
Au	1.48 ± 0.07	1.45
Nb	1.43 ± 0.06	1.43

and after the irradiation are presented in Fig. 3, and they clearly show that the 987.8 keV γ-ray peak is free of contributions from the sample activity. The second characteristic transition from the deexcitation of ^{240}Am at 888.9 keV is contaminated, therefore only the 987.8 keV transition was used for the cross-section analysis.

The absolute efficiency of the detectors for the reference foil measurements was obtained using a calibrated ^{152}Eu source placed at the same position as the samples. The decay data of the reference and Am targets are presented in Table II.

III. DATA ANALYSIS

The cross section of a reaction induced by a neutron with energy E_n is given by

$$\sigma = \frac{N_p}{N_\tau}\frac{1}{\Phi} \tag{1}$$

where N_p is the number of the nuclei produced during the irradiation, corrected for self-absorption and counting geometry, as well as for the decay of the product nuclide during the irradiation and the counting collection time. N_τ is the number of target nuclei and Φ is the time-integrated neutron flux over the irradiation time and is determined for Am targets by MCNP5 simulations, as mentioned before.

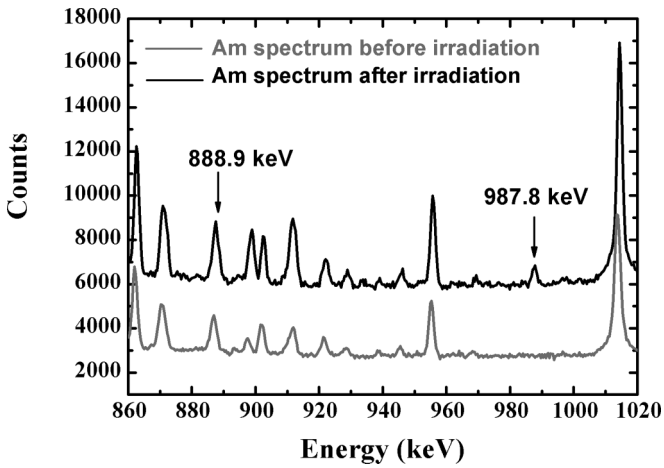

FIG. 3. High-energy part of the γ-ray spectra of an Am sample, before and after irradiation with 10.4 MeV neutrons.

TABLE II. Decay data of the ^{241}Am(n,2n)^{240}Am reaction along with those for the reference reactions [10].

Reaction	Q (MeV)	$T_{1/2}$	E_γ (keV)	I_γ (%)
^{241}Am(n,2n)^{240}Am	−6.65	50.8 h	987.8	73.2
^{27}Al(n,α)^{24}Na	−3.13	14.96 h	1368.6	100
^{197}Au(n,2n)^{196}Au	−8.07	6.18 d	355.7	87.0
^{93}Nb(n,2n)^{92m}Nb	−8.83	10.15 d	934.5	99.0

The integrated neutron flux Φ for the reference foils (shown in Table I) was determined with Eq. (1) by using the cross section values for the ^{27}Al(n,α)^{24}Na reaction from ENDF/B-VII.1, for the ^{197}Au(n,2n)^{196}Au reaction from TENDL 2012, and for the ^{93}Nb(n,2n)^{92m}Nb reaction by fitting the existing experimental data [11].

The number of the produced nuclei N_p has been determined by the expression

$$N_p = \frac{N_\gamma}{\varepsilon_\gamma F I_\gamma D f_c} \tag{2}$$

where N_γ is the number of γ-ray events recorded by the Ge detector, ε_γ is the efficiency of the Ge detector, and I_γ is the intensity of the characteristic transition. F is the total correction factor to account for self-absorption of the sample and counting geometry.

A correction factor which is a fraction of the produced nuclei that decay during irradiation is expressed by

$$f_c = \frac{\int_0^{t_B} e^{\lambda t} f(t) dt}{\int_0^{t_B} f(t) dt} e^{-\lambda \cdot t_B} \tag{3}$$

where t_B is the irradiation time.

The correction factor for the counting collection is given by the expression

$$D = e^{-\lambda t_1} - e^{-\lambda t_2} \tag{4}$$

where t_1 and t_2 are time intervals from the end of the irradiation to the beginning and finish of the measurement with the Ge detector, respectively, and λ is the decay constant of the residual nucleus.

Due to the complex geometry of the Am sample (Fig. 1), the efficiency of the detection setup along with the self-absorption effects [ε_γ and F factors in expression (2)] for the Am targets were extracted by using two different techniques: an experimental and a simulated one.

A. The experimental technique

The experimental technique, as described in Ref. [3], is based on the indirect evaluation of the factor F, through the determination of the ratio N_p/N_τ of Eq. (1) for the reaction ^{241}Am(n,2n)^{240}Am, from the gamma rays emitted by the irradiated americium sample. More specifically, while the number of produced nuclei is given by Eq. (2), the number of target (^{241}Am) nuclei is given by an equivalent relation,

without the f_c factor:

$$N_\tau = \frac{N'_\gamma}{\varepsilon' F' I'_\gamma D'} \tag{5}$$

Therefore, the ratio N_p/N_τ is given by the expression

$$\frac{N_p}{N_\tau} = \frac{N_\gamma}{I_\gamma}\frac{I'_\gamma}{N'_\gamma}\frac{D'}{D}\frac{1}{f_c}\frac{\varepsilon'}{\varepsilon}\frac{F'}{F} = R\frac{\varepsilon'}{\varepsilon}\frac{F'}{F} \tag{6}$$

The ratio R, as shown in Eq. (7), can be determined experimentally from the gamma rays emitted by the ^{241}Am target (N'_γ, I'_γ, and D' quantities) and the ^{240}Am produced nuclei (N_γ, I_γ, and D quantities). Since both are contained in the same sample, the γ rays used for the determination of the number of target and produced nuclei are subject to absorption by an identical matrix of materials in the americium target, in an identical source to detector geometry. For a fixed energy (for instance 987.8 keV), the overall correction factors F and F' and the detection efficiencies ε and ε' are therefore identical. Thus, the simplified expression of the ratio N_p/N_τ becomes

$$\frac{N_p}{N_\tau} = R = \frac{N_\gamma}{I_\gamma}\frac{I'_\gamma}{N'_\gamma}\frac{D'}{D}\frac{1}{f_c} \tag{7}$$

The R ratio has been evaluated experimentally by measuring N'_γ of several γ-ray lines emitted above 400 keV from the ^{241}Am of the sample, as well as N_γ of the 987.8 keV characteristic γ ray from the deexcitation of ^{240}Am. The intensities I_γ of the γ rays were taken from Ref. [10]. The results are shown in Fig. 4, from which the value of R for the energy 987.8 keV is taken by extrapolation and subsequently used for the cross section calculation using the equation

$$\sigma = R\frac{1}{\Phi} \tag{8}$$

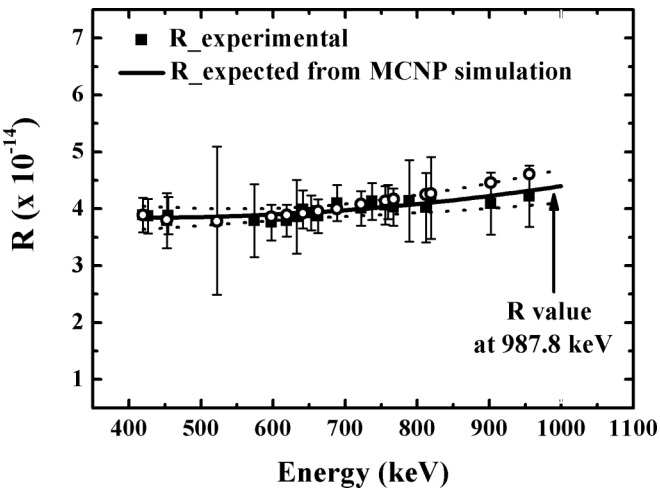

FIG. 4. Plot of the quantity R of Eq. (6), as a function of γ-ray energy taken at 10.4 MeV. The R value at 987.8 keV was determined by extrapolation. MCNP5 simulation results which indicate the dependence of ratio R from energy are also presented. The dotted curves denote the confidence bands.

In order to study the dependence of R on energy and the reliability of the fitting curve through the experimental points, MCNP5 simulations have been performed. The γ rays from the natural activity of Am have been introduced into the full geometry of the Am target setup and the HPGe detector. From the simulated γ-ray peaks the normalized R ratio has been deduced, and the results are shown as open circles in Fig. 4. The fair agreementbetween simulated and experimental points indicates that the second-order fitting curve is adequate to represent the energy dependence of R.

B. The simulated technique

According the Eqs. (1) and (2), the cross section is given by the expression

$$\sigma = \frac{N_\gamma}{N_\tau \Phi \varepsilon_\gamma F I_\gamma D f_c} \tag{9}$$

In this case, the efficiency of the Ge detector (ε_γ) along with the self-absorption correction factor (F) were deduced via a series of MCNP5 calculations which helped to fix the various geometrical parameters involved in the Am target assembly by reproducing the experimental spectra taken for different reference setups:

(a) HPGe detector and Eu point source to fix the detector,
(b) HPGe detector and Eu point source with the lead cylindrical box in front to fix the shielding,
(c) HPGe detector and Eu point source at the back of the lead cylindrical box with the Al container inside, to fix the container, and
(d) HPGe detector and Am pellet in its shielding before irradiation.

All these experimental spectra were reproduced fairly well (as shown in Table III) by the MCNP5 simulations and the deduced parameters of the detection setup were then used to simulate the ε_γ and F values for the 987.8 keV γ-ray transition, needed for the cross section calculation.

TABLE III. The experimental results for the detector's efficiency in comparison with the results from MCNP for the ^{241}Am target assembly [case (d)].

Energy of the photopeak (keV)	Counts in the experimental spectrum	Counts from MCNP simulation	Percentage difference (%)
332.36	3621000	3518600	2.83
335.38	11941400	11872800	0.57
368.59	5758700	5816250	−1.00
376.65	3790400	3779050	0.30
619.01	1753800	1794100	−2.30
688.72	904200	874800	3.25
722.01	5479300	5779300	−5.48

TABLE IV. Cross section values and uncertainties obtained from the two methods along with their weighted average results.

Neutron energy (MeV)	Experimental cross section σ (mb)	Cross section using MCNP simulation σ (mb)	Average cross section σ (mb)
10.0 ± 0.1	213 ± 18	182 ± 28	203 ± 15
10.4 ± 0.1	231 ± 21	227 ± 23	229 ± 16
10.8 ± 0.1	237 ± 22	238 ± 43	237 ± 20
17.1 ± 0.3	134 ± 11	142 ± 27	135 ± 11

C. Cross section values and uncertainties

The experimental results obtained from the two techniques (experimental and simulated) are presented in Table IV along with their uncertainties and weighted average values.

The final cross section values are shown in Fig. 5 compared with previous data and ENDF/B-VII.1 and JENDL-4.0 evaluations. The points around 10 MeV lie between the two evaluation data files.

The uncertainties were obtained by summing up quadratically all the possible individual errors that are summarized in Table V. More specifically, the uncertainty of the estimated neutron energy varied between 1–2%. In addition, a 4–5% uncertainty was assigned to the determination of the experimental neutron integrated flux, while 5% was considered the uncertainty in the neutron integrated flux deduced by MCNP5.

The uncertainty due to the counting statistics for the reference foils was 1%, but for the ^{240}Am peak the corresponding uncertainty was the most dominant (7–18%), due the low statistics of the 987.8 keV photopeak. Furthermore, the efficiency of the γ-ray detector had an uncertainty of about 3–4%. The uncertainty in the excitation function of the reference reactions was assumed to be 3%. Moreover, the uncertainty of the ratio R was estimated to be 7% according to the fitting curve reliability.

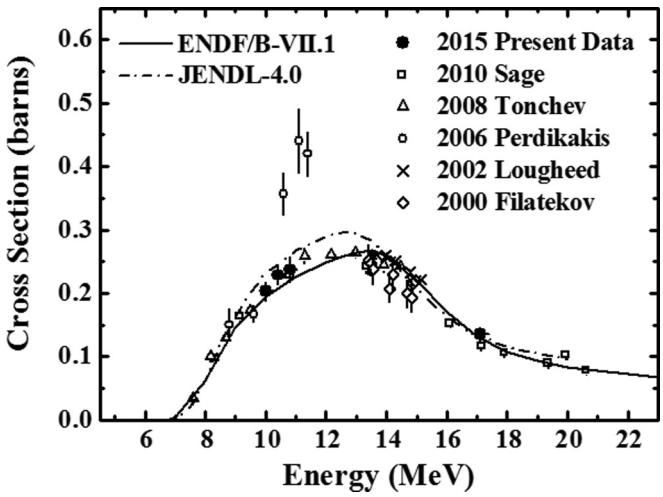

FIG. 5. The experimental ^{241}Am(n,2n)^{240}Am cross section values obtained at NCSR "Demokritos" compared with previous data and evaluations.

TABLE V. Compilation of uncertainties.

	Uncertainty (%)
Neutron energy[a,b]	1–2
Neutron integrated flux[a,b]	4–5
Neutron integrated flux from MCNP[a,b]	5
Counting statistics for reference foils[a,b]	1
Counting statistics for ^{240}Am peak[b]	7–18
Detector efficiency[a,b]	3–4
Reference reaction cross section[a,b]	3
R ratio[a]	7
Total uncertainty of cross section (σ_{exp})	9
Total uncertainty of cross section (σ_{MCNP})	10–19

[a]Contribute to the determination of σ_{exp}.
[b]Contribute to the determination of σ_{MCNP}.

Therefore, the total uncertainty in the case of the simulated technique was about 10–19%, and this is mainly attributed to the uncertainty of the counting statistics in the 987.8 keV photopeak, while in the case of the experimental technique the total estimated uncertainty is significantly reduced. This is due to the fact that the experimental technique, as shown in Fig. 4, represents a correlated analysis where the uncertainty does not exceed 7% at a confidence level equivalent to 4σ, as shown in Fig. 4.

IV. THEORETICAL CALCULATIONS

The cross section calculations were performed by means of the EMPIRE software package (version 3.2.2, "Malta") [12,13]. EMPIRE is a modular system of nuclear reaction codes implementing the major reaction mechanisms such as compound nucleus, preequilibrium emission, and direct.

Compound nucleus reaction calculations were performed in the framework of the Hauser-Feshbach theory [14] using suitable optical model potentials, nuclear level densities, and γ-ray strength functions available in the Reference Input Parameter Library (RIPL-3) database [15]. More specifically, the continuous excitation spectra of the nuclei at equilibrium deformation (nuclear level densities) were described by the Hartree-Fock-Bogoliubov microscopic model (HFBM), whereas the correlation between incident and exit channels in elastic scattering (width fluctuation corrections) was also taken into account according to the Hofmann-Richert-Tepel-Weidenmuller (HRTW) model [16]. The optical model parameters for outgoing particles were taken from RIPL using the data by Capote *et al.* [17].

Concerning the direct reactions, population of discrete collective levels in the inelastic scattering was calculated using the distorted-wave Born approximation (DWBA) method providing approximate direct cross sections (the ESIC06 code is used for that purpose), while optical model parameters used in DWBA calculations were taken from Maslov *et al.* [18].

Preequilibrium effects, whose impact increases with the neutron energy, were described by the exciton model [19] using the PCROSS code [20] for the calculations. In the present calculations neither multistep direct (MSD) calculations nor multistep compound (MSC) calculations were used because, as

TABLE VI. The final values used for the doubled-humped fission barriers description.

Nucleus Z	A	V_a (MeV)	h_a (MeV)	V_b (MeV)	h_b (MeV)
95	242	6.170	0.540	5.260	0.360
95	241	6.200	0.800	4.650	0.500
95	240	6.100	0.600	6.000	0.400
95	239	6.000	0.800	5.400	0.560

mentioned in Ref. [21], the combination of DWBA + PCROSS is an option which has an equivalent impact on the fission cross section with the MSD + MSC option.

The determination of the cross section for fission (n,f) on the ^{241}Am isotope plays a crucial role in the determination of the $(n,2n)$ reaction cross section, because fission is the main competing reaction channel to the latter. Therefore, the first step was to reproduce the existing experimental data in fission with adequate accuracy. For this purpose, the double-humped fission barrier model was implemented, whereas the Hartree-Fock-Bogoliubov combinatorial method described the level densities at saddle points. The parameters from the RIPL-3 empirical fission barriers were adopted as starting values, and subsequently adjusted to reproduce the bulk of experimental data. In order to accomplish this, it was not necessary to modify the RIPL-3 parameters by more than 13%. The final values used in the theoretical calculations are presented in Table VI. The description of the fission process did not require the implementation of discrete states above the fission barrier, while sub-barrier effects were taken into account, excluding isomeric fission and gamma emission inside the wells. Moreover, no recoils were calculated and the single modal fission approach proved to be adequate for this specific problem. For the remaining parameters the default values were adopted.

Eventually, by using the aforementioned parametrization, the EMPIRE code resulted in excellent reproduction of the existing experimental data in the fission channel [Fig. 6(a)] and at the same time, the calculations proved to be equally accurate for three more reaction channels: $(n,2n)$, $(n,3n)$ and (n,tot) [Figs. 6(b), 6(c), and 6(d) respectively].

V. RESULTS AND DISCUSSION

The mean cross section values from the two methods described before have been deduced, and the results for the ^{241}Am$(n,2n)^{240}$Am reaction cross section at 10.0, 10.4, 10.8, and 17.1 MeV are plotted in Fig. 6(a) along with existing data from literature and EMPIRE calculations.

Of the four cross section values obtained in this work, two can be compared with data from earlier measurements. These data points are at neutron energies 10.8 and 17.1 MeV. The former point is in excellent agreement with the data from Tochev *et al.* [4]. The latter point seems to agree within the experimental errors with the data from Sage *et al.* [5] in which the Am targets used come from the same batch of targets as those used in the present work. At the

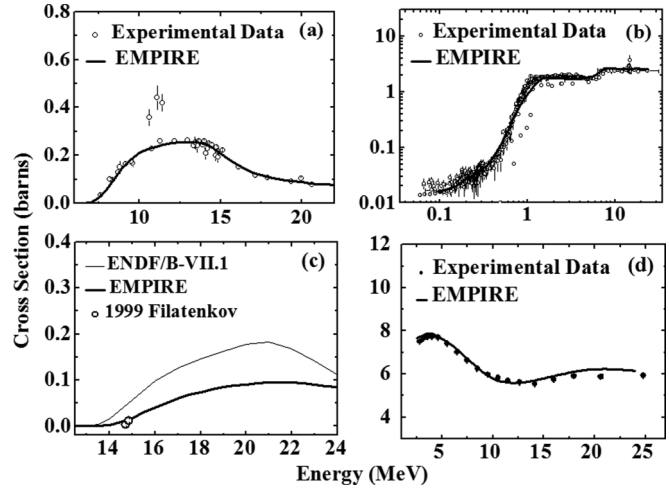

FIG. 6. Cross section of four reaction channels for the n + ^{241}Am interaction. Theoretical calculations results obtained with the EMPIRE code are presented along with the existing experimental data for each reaction: (a) ^{241}Am$(n,2n)$, (b) ^{241}Am(n,f), (c) ^{241}Am$(n,3n)$, (d) ^{241}Am(n,tot).

incident neutron energy range between 9.7 and 10.5 MeV, no other data are available. The two present data points at neutron energies 10.0 and 10.4 MeV seem to follow the general trend of the existing, neighboring data points [4,5] fairly well. Concerning the previous data measured at NCSR "Demokritos" by Perdikakis *et al.* [3], below 10 MeV the cross section values agree very well with the data of [4,5], while above 10 MeV they are significantly higher compared with the data of [4,5] and present results. Due to the significant presence of contaminants in the Am target used in that experiment [3], it is possible that above 10 MeV a neutron induced reaction on the contaminants of the target was open and produced a γ ray which interfered with the 987.8 keV transition, thus amplifying its yield and increasing the cross section value.

VI. CONCLUSIONS

The ^{241}Am$(n,2n)^{240}$Am reaction cross section has been measured in the incident neutron energy range between 10.0 and 17.1 MeV, relative to the ^{27}Al$(n,\alpha)^{24}$Na reaction reference cross section, using the activation technique. The motivation of these measurements was to resolve the discrepancies between the data by Perdikakis *et al.* [3] and by Tochev *et al.* [4], which agree below 10 MeV, while above 10 MeV they differ by a factor of about 2. The new measurements have been performed at the 5.5 MV Tandem T11/25 accelerator laboratory of NCSR "Demokritos", with high purity ^{241}Am targets provided by JRC-IRMM, Belgium. Due to the complex geometry of the Am sample, the efficiency of the detection setup, and the self-absorption correction for the Am, targets were extracted by using two different techniques: an experimental and a simulated one. The weighted average cross section values from both methods at 10.0, 10.4, and 10.8 MeV seem to agree with the data by Tonchev *et al.* [4] within their experimental

errors. The cross section value at 17.1 MeV seems to agree with the data by Sage *et al.* [5] within its experimental error. A possible explanation for the overestimated cross section values of previous data by Perdikakis *et al.* [3] is that a neutron-induced reaction on the contaminants of the target opens above 10 MeV and produces a γ ray which interferes with the 987.8 keV transition. Finally, a theoretical investigation of the ^{241}Am(n,2n) reaction cross section within the Hauser-Feshbach formalism with the EMPIRE code was performed, in the energy range 100 keV – 24 MeV, which also successfully reproduced the ^{241}Am(n,tot) as well as the ^{241}Am(n, f) and ^{241}Am(n,3n) competing reactions, in the corresponding energy region.

ACKNOWLEDGMENTS

Special thanks are due to A. Plompen for providing the Am targets produced at IRMM, as well as for his continuous interest in this work and many useful discussions. The invaluable assistance of the accelerator staff at the National Center for Scientific Researsch "Demokritos" is also gratefully acknowledged.

[1] A. A. Filatenkov and S. V. Chuvaev, Phys. At. Nucl. **63**, 1504 (2000).
[2] R. W. Lougheed *et al.*, Radiochim. Acta **90**, 833 (2002).
[3] G. Perdikakis, C. T. Papadopoulos, R. Vlastou, A. Lagoyannis, A. Spyrou, M. Kokkoris, S. Galanopoulos, N. Patronis, D. Karamanis, Ch. Zarkadas, G. Kalyva, and S. Kossionides, Phys. Rev. C **73**, 067601 (2006).
[4] A. P. Tonchev, C. T. Angell, M. Boswell, A. S. Crowell, B. Fallin, S. Hammond, C. R. Howell, A. Hutcheson, H. J. Karwowski, J. H. Kelley, R. S. Pedroni, W. Tornow, J. A. Becker, D. Dashdorj, J. Kenneally, R. A. Macri, M. A. Stoyer, C. Y. Wu, E. Bond, M. B. Chadwick, J. Fitzpatrick, T. Kawano, R. S. Rundberg, A. Slemmons, D. J. Vieira, and J. B. Wilhelmy, Phys. Rev. C **77**, 054610 (2008).
[5] C. Sage, V. Semkova, O. Bouland, P. Dessagne, A. Fernandez, F. Gunsing, C. Nästren, G. Noguère, H. Ottmar, A. J. M. Plompen, P. Romain, G. Rudolf, J. Somers, and F. Wastin, Phys. Rev. C **81**, 064604 (2010).
[6] E. Birgersson and G. Lovestam, JRC Science Hub Technical Report, Ref. No., 23794, 2009.
[7] J. F. Ziegler and J. P. Biersack, SRIM-2008. Available at http://www.srim.org.
[8] F. B. Brown, R. F. Barrett, T. E. Booth, J. S. Bull, L. J. Cox, R. A. Forster, T. J. Goorley, R. D. Mosteller, S. E Post, R. E. Prael, E. C. Selcow, A. Sood, and J. Sweezy, Trans. Am. Nucl. Soc. **87**, 273 (2002).
[9] X-5 Monte Carlo team, MCNP: A General Monte Carlo *N*-ParticleTransport Code, version 5, Volumes I–III, LA-UR-03-1987, LA-CP-03 0245, and LA-CP-03-0284, April 2003.
[10] R. B. Firestone and C. M. Baglin, *Table of Isotopes*, 8th ed. (John Wiley and Sons, New York 1999).
[11] https://www-nds.iaea.org/exfor.
[12] http://www.nndc.bnl.gov/empire/.
[13] M. Herman, R. Capote, B. V. Carlson, B. Oblozinsky, M. Sin, A. Trkov, H. Wienke, and V. Zerkin, Nucl. Data Sheets **108**, 2655 (2007).
[14] W. Hauser and H. Feshbach, Phys. Rev. **87**, 366 (1952).
[15] T. Belgya *et al.*, IAEA Technical Report No. IAEA-TECDOC-1506, 2006 (unpublished), available online at http://www.nds.iaea.org/RIPL-2/.
[16] H. M. Hofmann, J. Richert, J. W. Tepel, and H. A. Weidenmuller, Ann. Phys. (NY) **90**, 403 (1975).
[17] R. Capote, E. Soukhovitskii, S. Chiba, and J. M. Quesada, J. Nucl. Sci. Technol. Jpn. **45**, 333 (2008); Nice ND2007 Proceedings (paper no. 765).
[18] V. M. Maslov, Yu. V. Porodzinskij, N. A. Tetereva, M. Baba, and A. Hasegawa, Nucl. Phys. A **736**, 77 (2004).
[19] J. J. Griffin, Phys. Rev. Lett. **17**, 478 (1966).
[20] M. Herman, P. Oblozinsky, R. Capote, A. Trkov, V. Zerkin, M. Sin, and B. Carlson, http://www.nndc.bnl.gov/empire219.
[21] M. Sin, P. Oblozinsky, M. Herman, and R. Capote, J. Korean Phys. Soc. **59**, 1015 (2011).